

Model Adaptation for Inverse Problems in Imaging

Davis Gilton*, Gregory Ongie† and Rebecca Willett‡

November 4, 2021

Abstract

Deep neural networks have been applied successfully to a wide variety of inverse problems arising in computational imaging. These networks are typically trained using a forward model that describes the measurement process to be inverted, which is often incorporated directly into the network itself. However, these approaches lack robustness to drift of the forward model: if at test time the forward model varies (even slightly) from the one the network was trained for, the reconstruction performance can degrade substantially. Given a network trained to solve an initial inverse problem with a known forward model, we propose two novel procedures that adapt the network to a perturbed forward model, even without full knowledge of the perturbation. Our approaches do not require access to more labeled data (i.e., ground truth images), but only a small set of calibration measurements. We show these simple model adaptation procedures empirically achieve robustness to changes in the forward model in a variety of settings, including deblurring, super-resolution, and undersampled image reconstruction in magnetic resonance imaging.

1 Introduction

Repeated studies have illustrated that neural networks can be trained to solve inverse problems in imaging, including problems such as image reconstruction in MRI, inpainting, superresolution, deblurring, and more. Recent reviews and tutorials on this topic [4, 18] have described various approaches to this problem. In the general framework of interest, an unknown n -pixel image (in vectorized form) $x \in \mathbb{R}^n$ (or \mathbb{C}^n) is observed via m noisy measurements $y_0 \in \mathbb{R}^m$ (or \mathbb{C}^m) according to the model

$$y_0 = A_0 x + \varepsilon, \quad (1)$$

where A_0 is the *forward model* and ε represents a vector of noise. The goal is to recover x from y_0 .

In this paper, we focus on the setting in which the forward model A_0 is known and used during training. Past work has illustrated that leveraging knowledge of A_0 during training can reduce the sample complexity [9]. This paradigm is particularly common in applications such as medical imaging, where A_0 represents a model of the imaging system. For instance, in magnetic resonance imaging (MRI), A_0 reflects which k-space measurements are collected.

Unfortunately, these methods can be surprisingly fragile in the face of *model drift*, which occurs when, at test time, we are provided samples of the form

$$y_1 = A_1 x + \varepsilon \quad (2)$$

for some forward model $A_1 \neq A_0$. That is, assume we have trained a solver that is a function of both the original forward model A_0 and a learned neural network. One might try to reconstruct x from y_1 using this solver, and it will perform poorly because it is using a misspecified model (A_0 instead of A_1). Alternatively, we

*D. Gilton is with the department of Electrical and Computer Engineering at the University of Wisconsin-Madison, 1415 Engineering Dr, Madison, WI 53706 USA.

†G. Ongie is with the department of Mathematical and Statistical Sciences at Marquette University, 1250 W Wisconsin Ave, Milwaukee, WI 53233 USA.

‡R. Willett is with the Departments of Computer Science and Statistics at the University of Chicago, 5747 S Ellis Ave, Chicago, IL 60637 USA.

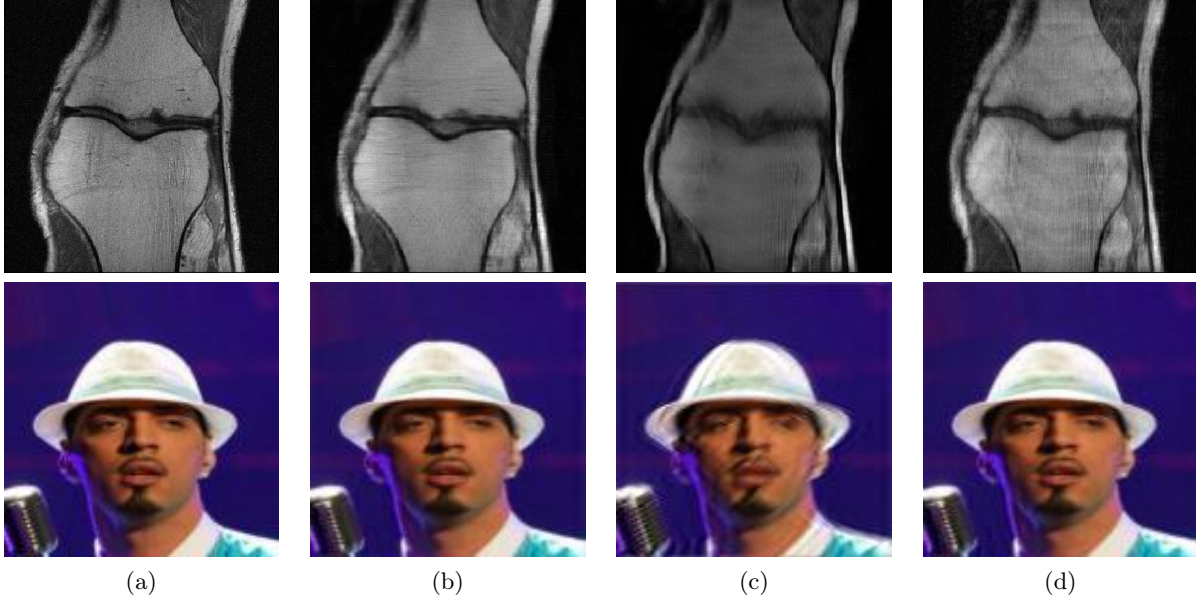


Figure 1: Small perturbations in measurements for deep learning-based image reconstruction operators can lead to both subtle and obvious artifacts in reconstructions across problems and domains. In the top row, we present results for undersampled MRI reconstruction of knee images, and the second row illustrates deblurring images of human faces. (a) Ground truth image. (b) No model drift. Training and test data correspond to same model, A_0 , yielding accurate reconstruction via learned model. (c) Model drift but no model adaptation. Training assumes model A_0 but at test time we have model A_1 . Reconstruction using trained network *without model adaptation* gives significant distortions. (d) Model drift and model adaptation. Training assumes model A_0 but at test time we have model A_1 . Reconstruction using model adaptation prevents distortions and compares favorably to the setting without model drift. Experimental details are in Section 4.

might attempt to use the same general solver where we replace A_0 with A_1 but leave the learned component intact. In this case, the estimate x computed from y_1 may also be poor, as illustrated in [3] and [14]. The situation is complicated even further if we do not have a precise model of A_1 at test time.

These are real challenges in practice. For example, in MRI reconstruction there is substantial variation in the forward model depending on the type of acquisition – e.g., Cartesian versus non-Cartesian k-space sampling trajectories, different undersampling factors, different number of coils and coil sensitivity maps, magnetic field inhomogeneity maps, and other calibration parameters [8] – all which need to be accounted for during training and testing. A network trained for one of these forward models may need to be retrained from scratch in order to perform well on even a slightly different setting (e.g., from four-fold to three-fold undersampling of k-space). Furthermore, training a new network from scratch may not always be feasible after deployment due to a lack of access to ground truth images. This could be either due to privacy concerns of sharing patient data between hospitals and researchers, or because acquiring ground truth images is difficult for the new inverse problem.

Model drift as stated above is a particular form of *distribution drift*, in which the distribution of $Y|X = x$ changes between training and deployment and we know Y has a linear dependence on X before and after the drift (even if we do not know the parameters of those linear relationships, represented as A_0 and A_1). To compute an accurate reconstruction under the original forward model, A_0 , the learned solver must reconstruct components of the image that lie in the null space $N(A_0)$: for superresolution, these are high-frequency details lost during downsampling, and in inpainting, these are the pixels removed by A_0 . Reconstructing under a different forward model, A_1 , requires reconstructing different components of the image in the null space $N(A_1)$. On top of this, components in the row space of A_0 that the solver uses to reconstruct x may lie in $N(A_1)$, causing further errors. As a toy example, consider a block-inpainting network trained to reconstruct the top quarter of an image: using this network to reconstruct the second-from-the-top quarter of an image will fail. Not only are the elements to reconstruct different ($N(A_1) \neq N(A_0)$), but the network will not have

learned how to use the top quarter of the image to reconstruct the rest.

These challenges lead us to formulate the problem of *model adaptation*: taking a reconstruction network trained for data resulting from forward model A_0 and adapting it to reconstruct images from measurements reflecting forward model A_1 . We consider two variants of this problem: (a) A_1 is known, along with a collection of unlabeled training samples $y_1^{(i)}$ reflecting A_1 , and (b) A_1 is *not* known, and we only have a collection of unlabeled training samples reflecting A_1 . These training samples are unlabeled in the sense that they are not paired with “ground truth” images used to generate the $y_1^{(i)}$ s. Our proposed model adaptation methods allow a reconstruction network to be trained for a known forward model and then adapted to related forward model without access to ground truth images, and without knowing the exact parameters of the new forward model.

1.1 Related Work

A broad collection of recent works, as surveyed by [4] and [18], have explored using machine learning methods to help solve inverse problems in imaging. The current paper is motivated in part by experiments presented in [3], which show that deep neural networks trained to solve inverse problems are prone to several types of instabilities. Specifically, they showed that model drift in the form of slight changes in the forward model (even “beneficial” ones, like increasing the number of k-space samples in MRI) often have detrimental impacts on reconstruction performance. While [3] is mostly empirical in nature, a follow-up mathematical study [10] provides theoretical support to this finding, implying that instability arises naturally from training standard deep learning inverse solvers.

To address a subset of these issues, [20] and [16] propose adversarial training frameworks that increases the robustness of inverse problem solvers. However, [20] and [16] focus on robustness to adversarial perturbations in the measurements for a fixed forward model, and do not address robustness to changes in the forward model, which is the focus of this work.

Similar to this work, a recent paper [12] has proposed domain adaptation techniques to transfer a reconstruction network from one inverse problem setting to another, e.g., adapting a network trained for CT reconstruction to perform MRI reconstruction. However, the focus of that approach is on adapting to *changes in the image distribution*, whereas our approaches focus on *changes to the forward model* assuming the image distribution is unchanged. Additionally, to our knowledge, no existing domain adaptation approaches consider the scenario where the new forward model depends on unknown calibration parameters, as we do in this work.

Another line of work explores learned methods for image reconstruction with automatic parameter tuning [23] and references therein; however, this work focuses on regularization and optimization parameters, not parameters of a drifting forward model. [24] describes a gradient unrolling approach to estimating a forward model, but in the sense of finding a forward model well-suited to the image distribution (over x ’s) rather than estimating the forward model used to generate data (the y s). Some recent studies have used pre-trained generative models to solve inverse problems with unknown calibration parameters [2]; this line of work can be viewed as an extension of compressed sensing with general models framework introduced in [6].

2 Problem Formulation

Suppose we have access to an estimator $\hat{x}_0 = f_0(y_0)$ that solves the inverse problem

$$y_0 = A_0x + \varepsilon, \quad x \sim P_x, \varepsilon \sim P_\varepsilon \quad (3)$$

where A_0 is a known (linear) forward model, P_x denotes the distribution of images x and P_ε denotes the distribution of noise ε . We assume the trained estimator “solves” the inverse problem in the sense that it produces an estimate $\hat{x}_0 = f_0(y_0)$ where the expected mean-squared error (MSE) $\mathbb{E}_{x,\varepsilon}[\|\hat{x}_0 - x\|^2]$ is small.

Now assume that the forward model has changed from A_0 to A_1 , resulting in a slightly different inverse problem

$$y_1 = A_1x + \varepsilon, \quad x \sim P_x, \varepsilon \sim P_\varepsilon. \quad (4)$$

Suppose we are given a new set of training measurements $\{y_1^{(i)}\}_{i=1}^N$ generated according to (4), but without access to paired ground truth images x_i . Our goal is to train a new estimator $\hat{x}_1 = f_1(y_1)$ to solve the new inverse problem.

We consider two cases: (a) The new forward model A_1 is known and (b) the new forward model A_1 is unknown, but assumed to be “close to” the original forward model A_0 in a sense made precise below.

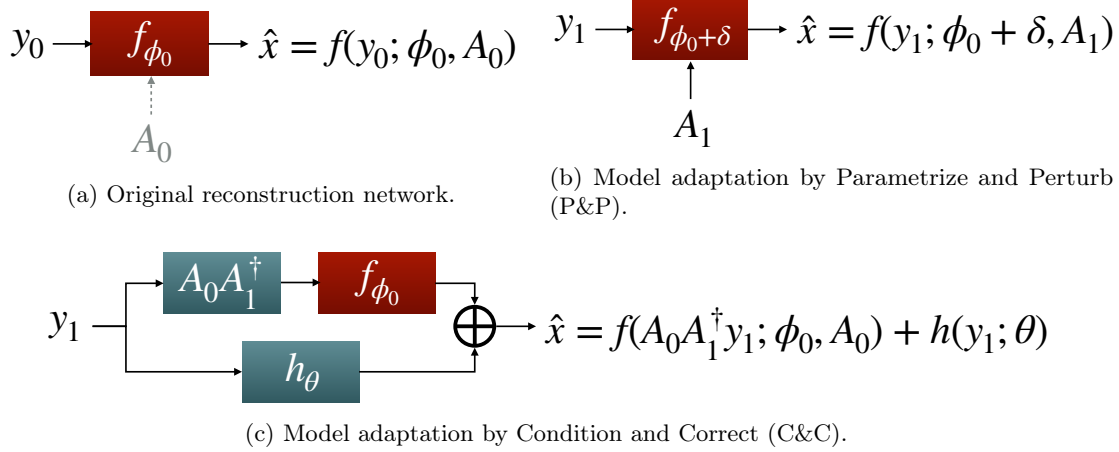


Figure 2: Three basic paradigms of reconstruction under “model drift”. (a) If the training data is generated using the model $y_0 = A_0 x + \epsilon$, this can be used to learn a reconstruction network $f(y_0; \phi_0, A_0)$ which is parameterized by weights or parameters ϕ_0 and may also explicitly depend on forward model A_0 . (b) **Parametrize and Perturb (P&P)**: If at test time we are presented with data corresponding to the model $y_1 = A_1 x + \epsilon$, we may not only use the new forward model A_1 but also perturb the parameters ϕ_0 to $\phi_1 = \phi_0 + \Delta$ to compensate for the model drift. (c) **Condition and Correct**: Alternatively to P&P, we may condition the input y_1 before it is fed into the original learned system from (a) and then learn a correction function h .

3 Proposed Approaches

We propose two distinct model adaptation approaches: *Parameterize & Perturb (P&P)* and *Condition & Correct (C&C)*.

3.1 Parametrize and Perturb: A network adaptation approach

First, we consider the case where we have knowledge of how the reconstruction network incorporates knowledge of A_0 (if at all). For instance, in the case for networks based on unrolling of iterative algorithms (see, for example, [4, 11, 17, 18, 22], and references therein), A_0 plays an explicit role. More generally, we assume an estimator of the form $\hat{x} = f(y; \phi, A)$ where y indicates input measurement and $\phi \in \mathbb{R}^q$ is a vector of network parameters. We also assume that the network has been trained to solve an inverse problem with a known forward model A_0 , resulting in the estimator $f_0(y) := f(y; \phi_0, A_0)$, where ϕ_0 is the vector of learned network parameters.

Given a set of new training measurements $\{y_1^{(i)}\}_{i=1}^N$, and a new forward model A_1 , we propose learning a new estimator $f_1(y) := f(y; \phi_1, A_1)$ where ϕ_1 is a new set of network parameters obtained by solving the optimization problem:

$$\min_{\phi} \sum_{i=1}^N \|y_1^{(i)} - A_1 f(y_1^{(i)}; \phi, A_1)\|^2 + \lambda \|\phi - \phi_0\|^2. \quad (5)$$

The proximity term $\|\phi - \phi_0\|^2$ ensures the new network parameters ϕ stay close to the original network parameters ϕ_0 . This term is necessary to avoid degenerate solutions, as demonstrated in Section 4.5.1. Note that by taking $\lambda \rightarrow \infty$ we enforce the constraint $\phi = \phi_0$. In this case, the resulting reconstruction network is given by $f(y; \phi_0, A_1)$, i.e., this is the “naive” approach, which changes A_0 to A_1 inside the reconstruction network, which can perform poorly as indicated in Figure 1.

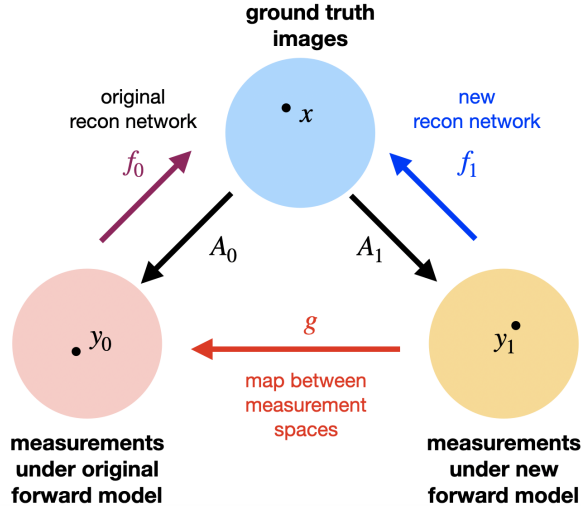


Figure 3: The relationship between the spaces discussed in this paper. In general, g , A_0 , and A_1 are all non-invertible; otherwise reconstruction is trivial.

If the forward model A_1 is also unknown, we propose optimizing for it as well in the above formulation, which gives:

$$\min_{\phi, A \in \mathcal{A}} \sum_{i=1}^N \|y_1^{(i)} - Af(y_1^{(i)}; \phi, A)\|^2 + \lambda \|\phi - \phi_0\|^2. \quad (6)$$

Directly optimizing (6) over all $m \times n$ matrices A is often impractical due to the large number of free parameters, and additional constraints on A are typically necessary. We assume the forward model is constrained to lie in a set $\mathcal{A} = \{A : A = A(\sigma)\}$, where $A(\sigma)$ is a forward model parametrized by $\sigma \in \mathbb{R}^q$ with $q \ll m \cdot n$ (e.g., in a deconvolution setting, $A(\sigma)$ represents convolution with an unknown kernel σ). We propose optimizing over $A \in \mathcal{A}$, which is possible with gradient methods, provided the map $\sigma \mapsto A_\sigma$ is first-order differentiable.

3.2 Condition and Correct: A network augmentation approach

Our second approach does not assume knowledge of how f might depend on A_0 ; in this case, directly replacing A_0 with A_1 as parameters of f is infeasible. We could still implement the P&P method in this setting, but it does not allow us to directly leverage knowledge of A_0 and A_1 when available. With this challenge in mind, we propose an alternative approach in which we map measurement y_1 to an estimate of what y_0 would have been if we'd observed x through forward model A_0 , applying our learned reconstruction network to this estimate of y_0 , and then adding in a correction term that is learned from the calibration data. We refer to this method as "Condition and Correct," or C&C.

One of the core criticisms of deep learned based reconstruction methods given in [3] is that adding more linear measurements at deployment than were considered during training (e.g., taking more k-space measurements in an MRI setting) results in lower-quality reconstructions. We formalize such a scenario by considering (for now) a scenario in which our new operator A_1 has its nullspace contained in the nullspace of A_0 , i.e., $N(A_1) \subset N(A_0)$. In this case, the new reconstruction network f_1 ought to obey

$$f_1(y_1) \approx f_0(g(y_1)). \quad (7)$$

where $g(\cdot)$ is any map that takes measurements $y_1 \in \mathbb{R}^{m_1}$ of an image under forward model A_1 to its corresponding measurement $y_0 \in \mathbb{R}^{m_0}$ under the forward model A_0 , i.e., $g(y_0) = y_1$. In particular, under the assumption $N(A_1) \subset N(A_0)$, we have $g(y) = A_0 A_1^\dagger y$ where A_1^\dagger is the pseudo-inverse of A_1 . In the context of MRI reconstruction, the constraint in (7) says that f_1 should not differ significantly from the hypothetical

system that discards the additional k-space data gathered under the measurement operator A_1 and instead solves the inverse problem using f_0 .

Above we assumed $N(A_1) \subset N(A_0)$. If this condition is violated (e.g., if A_0 and A_1 correspond to a sampling of k-space, where some k-space locations sampled in A_0 are not sampled in A_1), then in general $g(y_1) \neq y_0$. In this case, f_0 may return a reconstruction with unpredictable artifacts. Additionally, if the measurements contain noise, then $g(y_1)$ may have different noise statistics than what f_0 was trained on, which can also introduce artifacts.

To remedy this, we propose training an artifact removal network, $h(\cdot; \theta) : \mathbb{R}^m \rightarrow \mathbb{R}^n$ that maps from measurements to image space that is defined by network parameters θ , such that the new reconstruction network, f_1 is given by

$$f_1(y; \theta) = f_0(A_0 A_1^\dagger y) + h(y; \theta). \quad (8)$$

Using the representation of f_1 in (8), the constraint in (7) becomes $h(y_1, \theta) \approx 0$. Hence, we propose minimizing the training objective in terms of the network parameters θ :

$$\min_{\theta} \sum_{i=1}^N \left(\|A_1(f_0(A_0 A_1^\dagger y_1^{(i)}) + h(y_1^{(i)}; \theta)) - y_1^{(i)}\|_2^2 + \lambda \|h(y_1^{(i)}; \theta)\|_2^2 \right). \quad (9)$$

Additionally, if A_1 is unknown, we propose optimizing over it as well:

$$\min_{\theta, A \in \mathcal{A}} \sum_{i=1}^N \left[\|A \left(f_0(A_0 A^\dagger y_1^{(i)}) + h(y_1^{(i)}; \theta) \right) - y_1^{(i)}\|_2^2 + \lambda \|h(y_1^{(i)}; \theta)\|_2^2 \right]. \quad (10)$$

As in the previous section, if A has a known parameterization $A = A(\sigma)$ where $\sigma \in \mathbb{R}^q$ is a vector of parameters, we propose substituting this into (10) and optimizing over σ instead.

3.2.1 An approximation permitting simpler gradients

Optimizing (10) with respect to A requires differentiating through the pseudoinverse operation, which is challenging to do for a general matrix A . However, if we assume that $A = A_0 + \Delta$, where Δ is a small perturbation, then using a Neumann series expansion of the pseudoinverse [7], we have

$$A_0 A^\dagger y = A_0 (A_0 + \Delta)^\dagger y = \sum_{k=0}^{\infty} (-\Delta A_0^\dagger)^k y \approx \sum_{k=0}^m (-\Delta A_0^\dagger)^k y \quad (11)$$

If $\|\Delta\|$ is sufficiently small (in particular, if $\|\Delta\| \|A_0^\dagger\| < 1$), then the above sum converges rapidly and is well-approximated with few terms. Therefore, we propose replacing the terms $f_0(A_0 A^\dagger y_1^{(i)})$ in (10) with the approximation $f_0(\sum_{k=0}^m [(A - A_0) A_0^\dagger]^k y_1^{(i)})$, which is more easily back-propagated through. In our experiments, we use $m = 4$.

4 Experiments

In this section we empirically demonstrate our approach to model adaptation on three types of forward models with two example inverse problem solution methods. We have chosen these comparison points for their simplicity and to illustrate the broad applicability of our proposed approaches. In particular, our approaches to model adaptation are not tied to a specific architectural design.

4.1 Methods and Datasets Used

We demonstrate our approaches on three types of forward models: motion deblurring, superresolution, and undersampled MRI reconstruction. These forward models serve as an illustrative subset of possible real-world forward models.

For motion deblurring, our initial model A_0 corresponds to a 10° motion blur with a 7×7 kernel, and A_1 is a 15° motion blur with a 7×7 kernel, with angle given with respect to the horizontal axis. In superresolution,

our initial model is a bilinear downsampling with rate $2\times$, and A_1 corresponds to $2\times$ bicubic downsampling. MRI reconstruction is performed with an $8\times$ undersampled Cartesian pattern for both A_0 and A_1 . The sampling maps are shown in Fig 4.

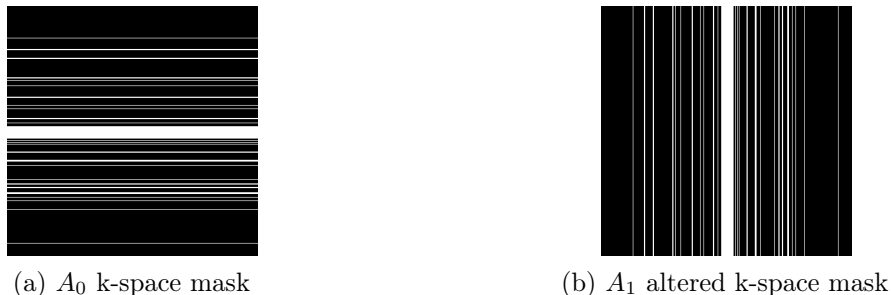


Figure 4: Visualization of k-space masks used for our MRI experiments. Each mask represents an 8-fold Cartesian undersampling with 4% of the center k-space lines fully sampled, an remaining lines sampled according to a Gaussian variable density scheme. The A_1 mask is a 90-degree rotation of the A_0 mask.

We use two datasets in our experiments. First, for motion deblurring and superresolution, we train and test on 128×128 -pixel aligned photos of human faces from the CelebA dataset [15]. The data used in the undersampled MRI experiments were obtained from the NYU fastMRI Initiative [26]. The primary goal of the fastMRI dataset is to test whether machine learning can aid in the reconstruction of medical images. We trained and tested on a subset of the single-coil knee dataset.

Learning rates and regularization parameters (λ in (5) and (9)) were tuned via cross-validation on a test set of 512 held-out images for CelebA, and 64 MRIs for fastMRI. Batch sizes were fixed in advance to be 128 for the motion blur and superresolution settings, and 8 for the MRI setting. Hyperparameters were tuned via grid search on a log scale. Empirically, we found a reasonable setting for λ is to choose λ such that the two loss terms in (5) and (9) are rescaled to be similar orders of magnitude.

The initial- and second-phase training sets are disjoint subsets of the original training set which are chosen at random. Unless otherwise noted, the initial- and second-phase training sets for CelebA contain 10^5 images, and the fastMRI sets contain 1000 MRI slices each.

We compare the performance of two architectures across all datasets. First, we utilize the U-Net architecture [21]. Our U-Net implementation takes as input the adjoint of the measurements under the forward model $A^\top y$, which is then passed through several CNN layers before obtaining a reconstructed image \hat{x} .

We also utilize the MoDL architecture [1], a learned architecture designed for solving inverse problems with known forward models. MoDL is an iterative or “unrolled” architecture, which alternates between a data-consistency step and a trained CNN denoiser, with weights tied across unrolled iterations. We use a U-Net architecture as the denoiser in our implementation of MoDL, ensuring that the number of parameters (except for a learned scaling factor in MoDL) in both of our approaches is the same.

4.2 Parametrizing forward models

Both proposed methods permit the new forward model to be unknown during training. In this case, the forward model is learned along with the new reconstruction method. Here we describe the parametrization that is used.

For the deblurring task, the unknown blur kernel is parametrized as a 7×7 blur kernel, initialized with the weights used for the ground-truth kernel during the initial stage of training. Practically this is identical to a standard convolutional layer with a special initialization and only one learned kernel.

A similar approach is used for superresolution. The forward model can be efficiently represented by strided convolution, and the adjoint is represented by a standard “convolution transpose” layer, again with the weights initialized to match the forward operator in the initial pre-training phase.

In the case of MRI with a Cartesian sampling of k-space, the forward model (i.e., the set of k-space sampling locations) is typically known to a high degree of accuracy at acquisition time, so we do not attempt

		Baselines			Proposed Model Adaptation Methods				
		Train w/ A_0	Train w/ A_1	Train w/ A_0	Known A_1		Unknown A_1		
		Test w/ A_0	Test w/ A_1	Test w/ A_1	P&P (Eq. 5)	C&C (Eq. 9)	P&P (Eq. 6)	C&C (Eq. 10)	
Motion Blur	U-Net	33.8- 34.1 -34.3	34.0- 34.3 -34.6	27.9- 28.1 -28.3	32.5- 32.8 -33.0	32.0- 32.3 -32.7	30.4- 30.6 -30.8	31.1- 31.3 -31.6	
	MoDL	35.5- 36.2 -36.8	35.3- 36.1 -36.7	23.7- 24.2 -24.7	33.2- 33.7 -34.4	35.0- 35.6 -36.2	33.1- 33.6 -34.1	33.4- 34.1 -34.9	
Superresolution	U-Net	29.9- 30.2 -30.4	27.9- 28.1 -28.4	19.1- 19.3 -19.5	26.2- 26.5 -26.7	24.9- 25.2 -25.5	23.3- 25.0 -26.0	23.9- 25.7 -26.5	
	MoDL	29.9- 30.5 -31.1	26.3- 26.8 -27.3	18.5- 18.8 -19.1	27.1- 28.1 -28.5	27.6- 28.2 -28.8	25.0- 27.0 -28.9	24.4- 27.2 -28.4	
MRI	U-Net	29.0- 29.7 -30.5	29.2- 30.3 -30.9	25.4- 26.1 -26.9	28.9- 29.6 -30.1	28.8- 29.8 -30.6	-	-	
	MoDL	30.3- 31.4 -32.4	31.6- 32.6 -33.3	4.1- 4.5 -5.3	29.6- 30.8 -31.6	28.8- 29.9 -30.6	-	-	

Table 1: Comparison of proposed model adaptation approaches across a variety of datasets and forward models. **Bolded** numbers indicate the median PSNR across the test set, and numbers before and after the median indicate the PSNR at the 25th and 75th percentile respectively.

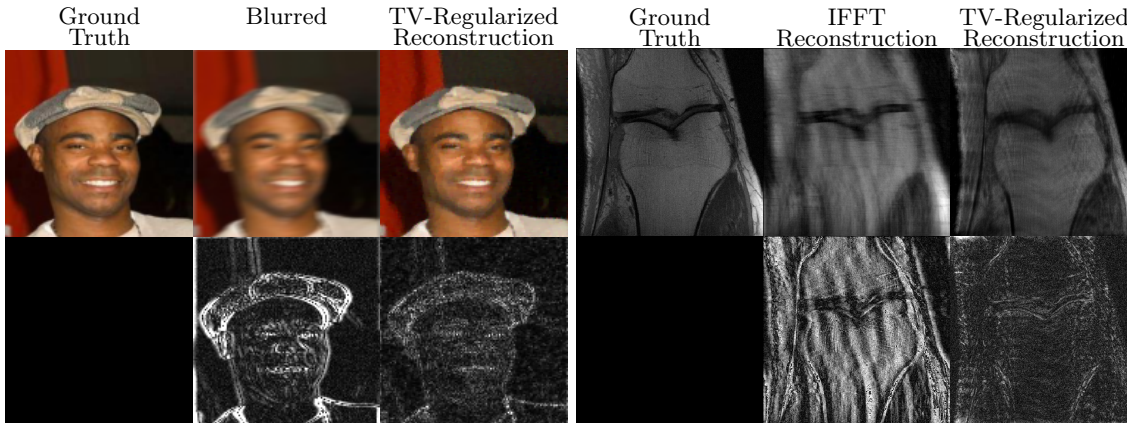


Figure 5: Comparison figures for the deblurring methods in Figure 6 and the MRI reconstruction methods in Figure 7. For deblurring, we present the ground truth, the blurred image (with Gaussian noise with $\sigma = 0.01$ added), and a sample total-variation regularized reconstruction (with PSNR 33.2 dB). For MRI, we present the IFFT with all k-space data maintained, the naïve IFFT reconstruction after k-space masking, and a sample total-variation regularized reconstruction (with PSNR 27.3 dB). We also present the residuals relative to the no-masking IFFT, multiplied by $5\times$ for ease of visualization.

to learn a new forward model for the MRI reconstruction approach.

4.3 Main results

In Table 1 we present our main results. We present sample reconstructions for the deblurring problem and MRI reconstruction problem in Figs. 6 and 7. For reference, the ground truth, inputs to the networks, and a total variation regularized reconstruction are presented in Fig. 5.

While the magnitude of the improvements vary across domains and problems, we find that retraining the network with the proposed model adaptation techniques significantly improve performance by several dBs in the new setting. This effect is particularly striking in the case MRI reconstruction with MoDL, where the “naïve” approach of replacing A_0 with A_1 in the network gives catastrophic results (median reconstruction error 5dB PSNR), while the proposed model adaptation approaches give reconstruction errors on par with both training and testing with A_0 or A_1 (roughly 30 dB).

Our experiments show no clear winner between C&C and P&P for all inverse problems/architectures. In our experiments on MRI reconstruction C&C performs best, while for motion blur and superresolution with a known forward model A_1 , P&P performs best. However, in scenarios with an unknown forward model A_1 , the C&C approach performed best.

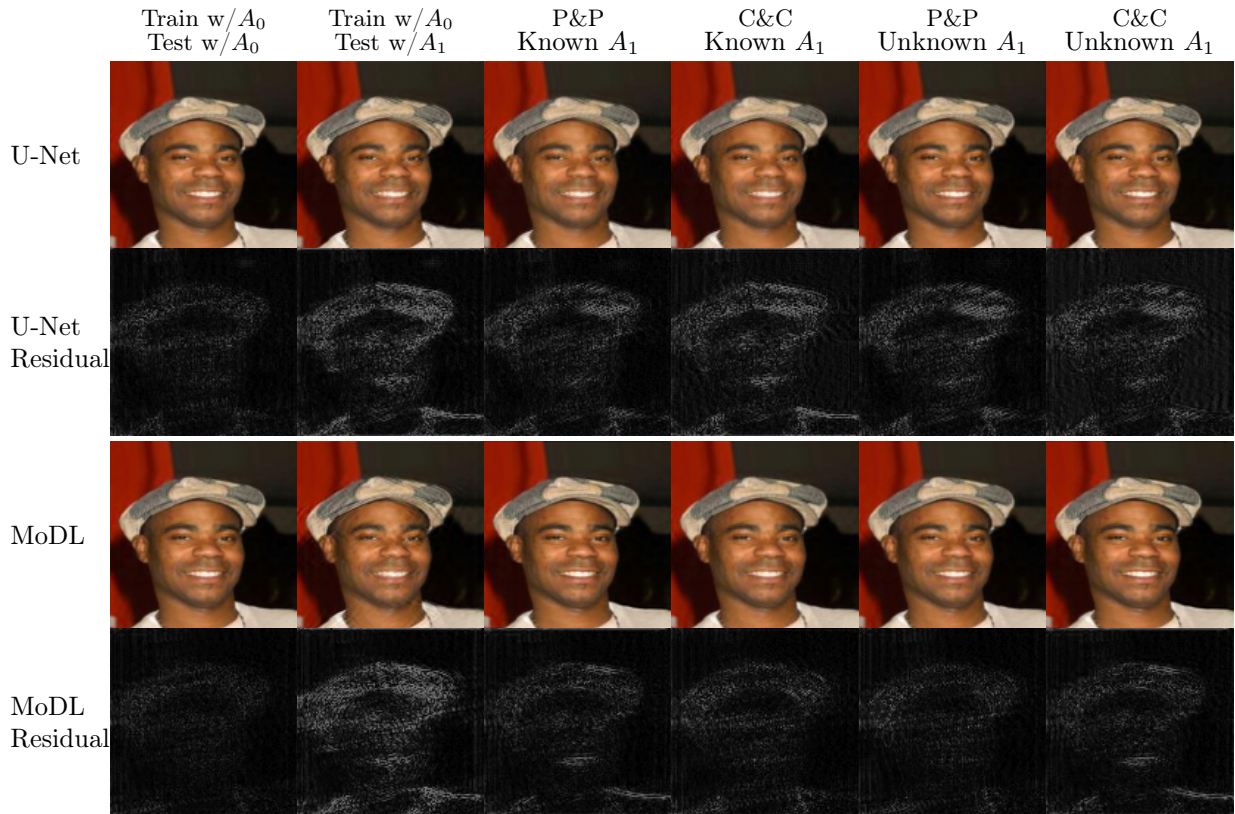


Figure 6: Visual examples of reconstruction quality for the motion deblurring inverse problem solved by U-Net and MoDL, as well as the associated residuals. Each residual is multiplied by 5 for ease of inspection. The initial forward model A_0 is a 5×5 motion blur with angle 10° , and the A_1 model has a 5×5 motion blur kernel with angle 15° . The analogous figure for the superresolution problem, and further examples, are available in the Supplement. Best viewed electronically.

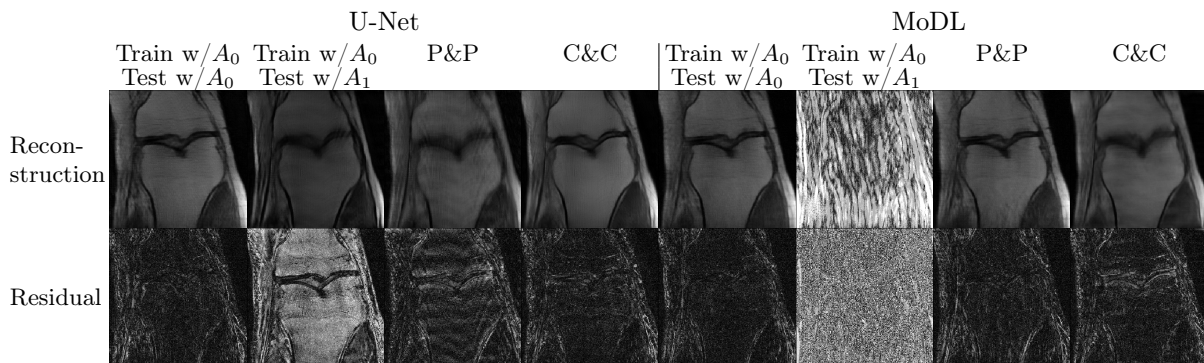


Figure 7: Visual examples of different reconstruction approaches for the MRI inverse problem under model drift, along with associated residuals. All residual images are scaled by 5x for ease of inspection. Best viewed electronically.

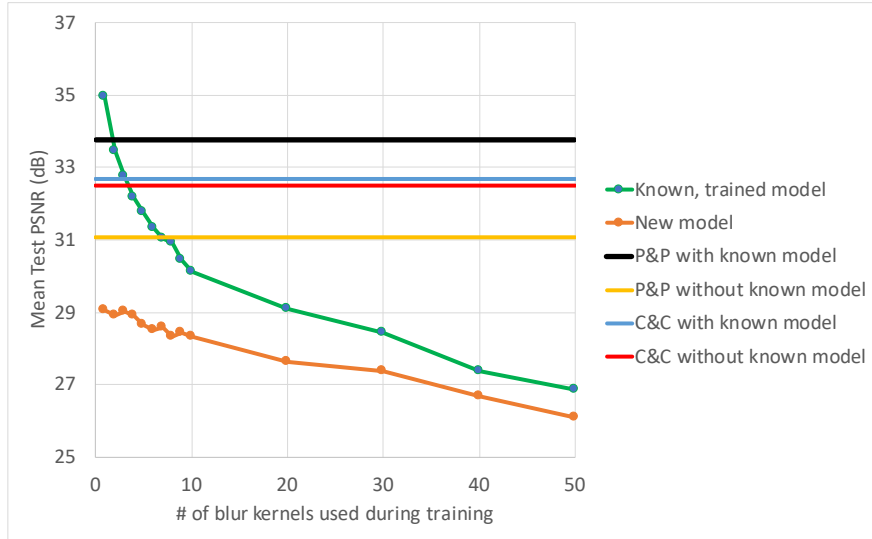


Figure 8: Naïvely learning to deblur with a single network and multiple blur kernels sacrifices performance on all blurs. In **green**, the test-time accuracy of a network trained to deblur multiple blurs, tested on a known kernel. In **orange**, the same network, but tested on a new blur that was not used during training. In **black**, our proposed P&P approach (Eq. 6), with a known model, and in **yellow** the same with a learned forward model. **Blue** and **red** show the performance of our C&C approach (Eq. 10), with and without a known forward model.

4.4 Learning multiple forward models

In this section we explore an alternative approach to model adaptation. In this setting, we assume that a set of candidate forward models are known during training time. During test time, a single forward model is used for measurement, but the test-time forward model is not known during training. This case represents the setting where the forward model might be parametrized, and so a reasonable approach may be to train the learned network using a number of different forward models to improve robustness.

In simple settings, training on multiple models might be reasonable. However, when the forward model parameterization is high-dimensional, learning to invert all possible forward models may be difficult.

We demonstrate this setting with a deblurring example, in which the same network is trained using a number of blur kernels. The forward blur kernels are the same kernels used for comparisons in [13]. For consistency, we resize all 50 blur kernels to 7x7, and normalize the weights to sum to 1. We compare reconstruction accuracy when the ground truth blur kernel is included in the set of kernels used for training, as well as when the reconstruction network has never seen data blurred with the testing kernel.

The results are shown in Fig 8. Experimentally, we find that training on multiple blur kernels simultaneously incurs a performance penalty as the number of blur kernels used in training increases. In this setting, where the forward model has many degrees of freedom and data is limited, attempting to learn to solve all models simultaneously is worse than transferring a single learned model, even in the absence of further ground truth data for calibration.

4.5 Proximity loss study and examination of learned components

In this section we explore further details of the learned methods. We first examine the effect of training without the proximity term in the adaptation loss of (5), demonstrating that just refitting the data without staying close to the original model is not enough. We then explore whether our trained models learn accurate forward models by examining the blur kernels learned during training.



Figure 9: Role of proximity term in model adaptation for motion deblurring with P&P (Eq. (5)). When ablating the term that promotes proximity to the initial network weights in the P&P approach ($\lambda = 0$ in (5)), the retrained network outputs degenerate solutions that match the measurements (center row), but lack fidelity with the ground truth (top row). By including the proximity term ($\lambda \neq 0$ in (5)), we learn a small corrective perturbation to the network weights that improves reconstruction accuracy significantly (bottom row).

4.5.1 Ablating the proximity term

In Figure 9 we demonstrate the effect of ablating the proximity term in (5), which we believe are necessary to avoid degenerate solutions. Optimizing (5) or (9) without proximity terms fails to leverage the network learned for A_0 using ground truth images x . Without the proximity term, our solution relies too heavily on the calibration data without ground truth information. We empirically find the proximity term is necessary to maintain good reconstructions.

4.5.2 Learned blur kernels

In Figure 10 we illustrate the true original, true new, and learned approximations from the P&P and C&C approaches. The U-net reconstruction kernel estimate is closer to the ground truth kernel than the kernel learned by MoDL, although the MoDL reconstructions have better PSNR. Similarly, the C&C method of retraining MoDL has a less accurate estimate of the blur kernel than P&P, but higher PSNR.

4.6 Sample Complexity

In the transfer learning setting, a key concern is the size of the transfer learning set necessary to achieve high-quality results. In this section we compare the performance of our approaches across different sample sizes.

In Fig. 12 we explore the effect of the number of samples observed under the new forward model on the adapted model. We observe that even without knowing the forward model, only two calibration samples are required to observe an improvement over a method that replaces A_0 with A_1 without further retraining. When the forward model is known during calibration and testing, a single example image can result in a 2 dB improvement in PSNR.

4.7 Model-Blind Reconstruction with Generative Networks

Recent work [2,5,6] has explored solving inverse problems using generative networks, which permit reconstruction under arbitrary forward models assuming an expressive enough generative network. In particular, [2] and [5] consider the case where the forward model is either partially or entirely unknown, and hence may be

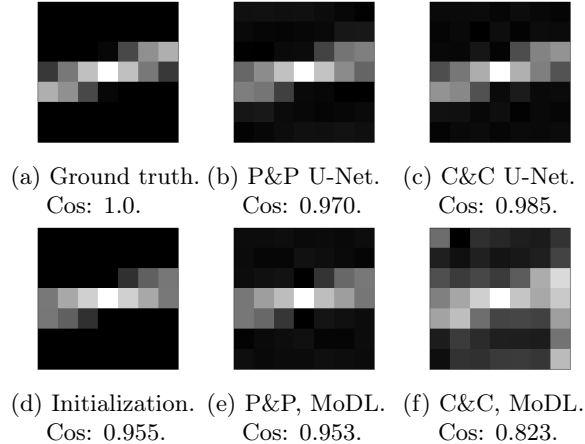


Figure 10: Learned blur kernels for the different model adaptation techniques/architectures. Below each kernel is the cosine similarity to the ground-truth kernel, shown in (a). The optimization is always initialized to the original kernel, shown in (d). The learned blur kernels vary significantly in quality across settings: the C&C approaches, shown in (c) and (f), tend to alter the learned kernel during training more than the P&P approaches, shown in (b) and (e).

learned by parameterizing and jointly optimizing over both the forward model and the latent code for the generative network.

In Fig. 11 we provide an illustration of reconstructions obtained by the method of [2], compared to our proposed C&C approach, with an unknown forward model. In our demonstration, as in [2], the generative network under consideration is a pretrained DCGAN [19]. For both deblurring and superresolution, the reconstruction quality is significantly higher when a model-specific network is used, and the image quality of the generative approach is low.

In the absence of (x_i, y_i) pairs, a generative approach may be reasonable. However, learning the data manifold in its entirety requires a great deal of data at minimum, along with a sufficiently large and well-tuned generator. The authors of [25] also note this fundamental limitation: for smaller or simpler applications, learning a high-quality GAN is straightforward, but for more complex applications it is difficult to train GAN models that are sufficiently accurate to rely on for reconstruction.

5 Discussion and Conclusion

This paper explores solutions to the fragility of learned inverse problem solvers in the face of model drift. We demonstrate across a range of simple, practical applications that using a learned model in settings even slightly different than they were trained in results in significant reconstruction errors, both subtle and obvious. We propose two calibration procedures: the first learns a perturbation to the learned network parameters, which we call Parametrize and Perturb (P&P); the second conditions the input on the new forward model and learns a correction to the learned network, which we call Condition and Correct (C&C).

We show that our calibration techniques can enable reuse of learned solvers in novel settings, even when the new forward model is not known. In addition, we demonstrate that just learning to invert many models is not the solution to the problem of robustness: directly learning many models empirically appears to cause reconstruction quality to fall across all learned models. We also show that our approach is superior to one that requires learning a model of the entire image space via a generative model.

Retraining learned inverse problem solvers to function under new forward models is just one step towards robustifying these powerful approaches to real-world deviations. Our approach for unknown A_1 relies on learning new parameters for a forward model, but such a parametrization is not always straightforward or realistic. How best to adapt to complex changes in the forward model that are not easily parametrized is an important open question for future work. In addition, we have addressed model drift, but an important open problem is determining how to adapt to simultaneous model and data distribution drift across settings. We

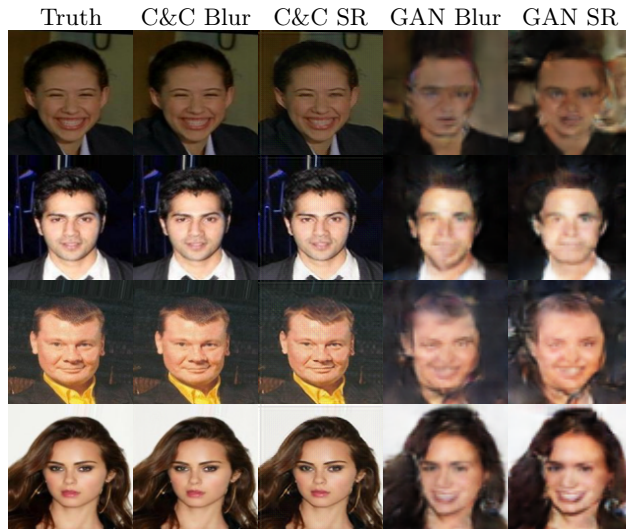


Figure 11: Comparison of model adaptation (C&C) with a model-blind GAN-based reconstruction approach for motion deblurring (Blur) and super-resolution (SR). While a GAN-based approach only requires learning a single generative network for all forward models, our results suggest that a network trained for a specific forward model with same number training samples typically has higher reconstruction accuracy, as illustrated above. Best viewed electronically.

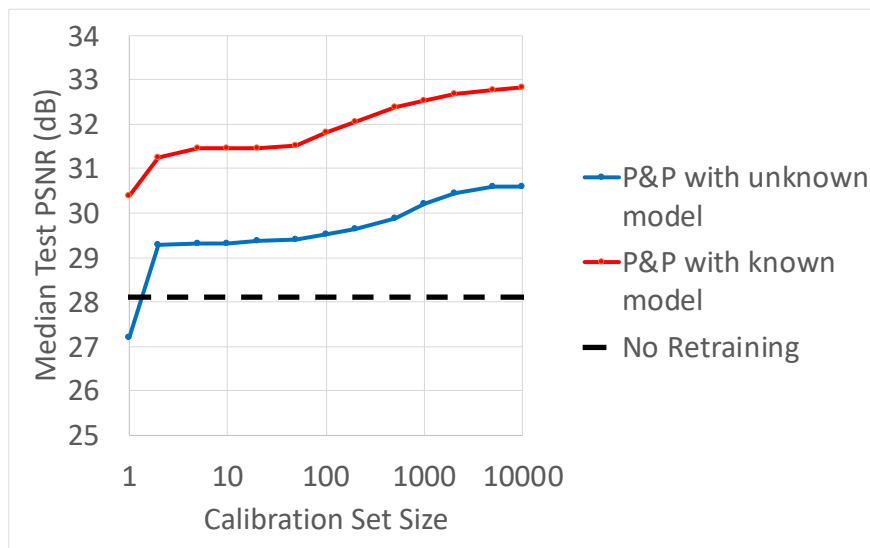


Figure 12: Performance of the P&P model adaptation approach for motion deblurring as a function of the number of training samples (blurred images) under the new forward model. For our approaches, only two samples are required to outperform a naive approach that does not retrain, even without exact knowledge of the new forward model. When the new forward model is known, tuning the network with even a single training example results in a 2.5 dB increase in PSNR.

hope to address these questions in future work.

References

- [1] Hemant K Aggarwal, Merry P Mani, and Mathews Jacob. MoDL: Model-based deep learning architecture for inverse problems. *IEEE transactions on medical imaging*, 38(2):394–405, 2018.
- [2] Rushil Anirudh, Jayaraman J Thiagarajan, Bhavya Kailkhura, and Timo Bremer. An unsupervised approach to solving inverse problems using generative adversarial networks. *arXiv preprint arXiv:1805.07281*, 2018.
- [3] Vegard Antun, Francesco Renna, Clarice Poon, Ben Adcock, and Anders C Hansen. On instabilities of deep learning in image reconstruction and the potential costs of ai. *Proceedings of the National Academy of Sciences*, 2020.
- [4] Simon Arridge, Peter Maass, Ozan Öktem, and Carola-Bibiane Schönlieb. Solving inverse problems using data-driven models. *Acta Numerica*, 28:1–174, 2019.
- [5] Kalliopi Basioti and George V Moustakides. Image restoration from parametric transformations using generative models. *arXiv preprint arXiv:2005.14036*, 2020.
- [6] Ashish Bora, Ajil Jalal, Eric Price, and Alexandros G Dimakis. Compressed sensing using generative models. In *Proceedings of the 34th International Conference on Machine Learning-Volume 70*, pages 537–546. JMLR. org, 2017.
- [7] Joan-Josep Climent, Néstor Thome, and Yimin Wei. A geometrical approach on generalized inverses by neumann-type series. *Linear algebra and its applications*, 332:533–540, 2001.
- [8] Jeffrey A Fessler. Model-based image reconstruction for MRI. *IEEE signal processing magazine*, 27(4):81–89, 2010.
- [9] Davis Gilton, Greg Ongie, and Rebecca Willett. Neumann networks for linear inverse problems in imaging. *IEEE Transactions on Computational Imaging*, 2019.
- [10] Nina M Gottschling, Vegard Antun, Ben Adcock, and Anders C Hansen. The troublesome kernel: why deep learning for inverse problems is typically unstable. *arXiv preprint arXiv:2001.01258*, 2020.
- [11] Karol Gregor and Yann LeCun. Learning fast approximations of sparse coding. In *Proceedings of the 27th international conference on international conference on machine learning*, pages 399–406, 2010.
- [12] Yoseob Han, Jaejun Yoo, Hak Hee Kim, Hee Jung Shin, Kyunghyun Sung, and Jong Chul Ye. Deep learning with domain adaptation for accelerated projection-reconstruction mr. *Magnetic resonance in medicine*, 80(3):1189–1205, 2018.
- [13] Michal Hradiš, Jan Kotera, Pavel Zemcik, and Filip Šroubek. Convolutional neural networks for direct text deblurring. In *Proceedings of BMVC*, volume 10, page 2, 2015.
- [14] Shady Abu Hussein, Tom Tirer, and Raja Giryes. Correction filter for single image super-resolution: Robustifying off-the-shelf deep super-resolvers. In *Proceedings of the IEEE/CVF Conference on Computer Vision and Pattern Recognition*, pages 1428–1437, 2020.
- [15] Ziwei Liu, Ping Luo, Xiaogang Wang, and Xiaoou Tang. Deep learning face attributes in the wild. In *Proceedings of International Conference on Computer Vision (ICCV)*, December 2015.
- [16] Sebastian Lunz, Ozan Öktem, and Carola-Bibiane Schönlieb. Adversarial regularizers in inverse problems. In *Advances in Neural Information Processing Systems*, pages 8507–8516, 2018.
- [17] Morteza Mardani, Qingyun Sun, David Donoho, Vardan Papayan, Hatef Monajemi, Shreyas Vasanawala, and John Pauly. Neural proximal gradient descent for compressive imaging. In *Advances in Neural Information Processing Systems*, pages 9573–9583, 2018.

- [18] Gregory Ongie, Ajil Jalal, Christopher A Metzler, Richard G Baraniuk, Alexandros G Dimakis, and Rebecca Willett. Deep learning techniques for inverse problems in imaging. *arXiv preprint arXiv:2005.06001*, 2020.
- [19] Alec Radford, Luke Metz, and Soumith Chintala. Unsupervised representation learning with deep convolutional generative adversarial networks. *arXiv preprint arXiv:1511.06434*, 2015.
- [20] Ankit Raj, Yoram Bresler, and Bo Li. Improving robustness of deep-learning-based image reconstruction. *arXiv preprint arXiv:2002.11821*, 2020.
- [21] Olaf Ronneberger, Philipp Fischer, and Thomas Brox. U-net: Convolutional networks for biomedical image segmentation. In *International Conference on Medical image computing and computer-assisted intervention*, pages 234–241. Springer, 2015.
- [22] Jian Sun, Huibin Li, Zongben Xu, et al. Deep ADMM-Net for compressive sensing MRI. In *Advances in neural information processing systems*, pages 10–18, 2016.
- [23] Kaixuan Wei, Angelica Aviles-Rivero, Jingwei Liang, Ying Fu, Carola-Bibiane Schnlieb, and Hua Huang. Tuning-free plug-and-play proximal algorithm for inverse imaging problems. *arXiv preprint arXiv:2002.09611*, 2020.
- [24] Shanshan Wu, Alex Dimakis, Sujay Sanghavi, Felix Yu, Daniel Holtmann-Rice, Dmitry Storcheus, Afshin Rostamizadeh, and Sanjiv Kumar. Learning a compressed sensing measurement matrix via gradient unrolling. In *International Conference on Machine Learning*, pages 6828–6839. PMLR, 2019.
- [25] Raymond A Yeh, Chen Chen, Teck Yian Lim, Alexander G Schwing, Mark Hasegawa-Johnson, and Minh N Do. Semantic image inpainting with deep generative models. In *Proceedings of the IEEE conference on computer vision and pattern recognition*, pages 5485–5493, 2017.
- [26] Jure Zbontar, Florian Knoll, Anuroop Sriram, Matthew J. Muckley, Mary Bruno, Aaron Defazio, Marc Parente, Krzysztof J. Geras, Joe Katsnelson, Hersh Chandarana, Zizhao Zhang, Michal Drozdal, Adriana Romero, Michael Rabbat, Pascal Vincent, James Pinkerton, Duo Wang, Nafissa Yakubova, Erich Owens, C. Lawrence Zitnick, Michael P. Recht, Daniel K. Sodickson, and Yvonne W. Lui. fastMRI: An open dataset and benchmarks for accelerated MRI. 2018.